GeRnika: An R Package for the Simulation, Visualization and Comparison of Tumor Phylogenies

by A. Sánchez-Ferrera[*]*, M. Tellaetxe-Abete*[*]*, B. Calvo-Molinos*

Abstract The development of methods to study intratumoral heterogeneity and tumor phylogenies is a highly active area of research. However, the advancement of these approaches often necessitates access to substantial amounts of data, which can be challenging and expensive to acquire. Moreover, the assessment of results requires tools for visualizing and comparing tumor phylogenies. In this paper, we introduce GeRnika, an R package designed to address these needs by enabling the simulation, visualization, and comparison of tumor evolution data. In summary, GeRnika provides researchers with a user-friendly tool that facilitates the analysis of their approaches aimed at studying tumor composition and evolutionary history.

1 Introduction

The development of tumors is a complex and dynamic process characterized by a succession of events where DNA mutations accumulate over time. These mutations give rise to genetic diversity within the tumor, leading to the emergence of distinct clonal subpopulations or, simply, clones (Nowell, 1976). Each of these subpopulations exhibits unique mutational profiles, resulting in varied phenotypic and behavioral characteristics among the cancer cells (Marass et al., 2016). This phenomenon, known as intratumoral heterogeneity (ITH), significantly hinders the design of effective medical therapies, since different clones within the same tumor may respond differently to treatments, ultimately leading to therapy resistance and disease recurrence (Burrell et al., 2013). To address this challenge, several innovative approaches are being developed to study the tumor composition in greater detail and to reconstruct its evolutionary history.

One common approach to studying tumor composition and phylogeny involves using bulk DNA sequencing data from multiple tumor biopsies. This data is relatively straightforward to obtain and provides a broad overview of the genetic alterations within the tumor. However, using bulk sequencing data in the study of ITH faces the challenge that each sample potentially contains a mixture of different clonal populations rather than just one clone. Consequently, the observed mutation frequencies—measured as variant allele frequencies (VAFs)—do not directly estimate the fraction of individual clones. Instead, the VAF values represent a composite signal: the sum of the fractions of all clones that harbor each mutation in a given sample.

This complexity implies that reconstructing the tumor's evolutionary history requires deconvolving these clonal admixtures within the samples. This task is precisely the focus of the Clonal Deconvolution and Evolution Problem (CDEP) (Strino et al., 2013; El-Kebir et al., 2015), which can be summarized as determining the tumor's clonal structure—that is, identifying the number, proportion, and mutational composition of clones in each sample—as well as reconstructing the clonal phylogenetic tree that leads to the observed clonal mosaic. In this context, one of the most prominent approaches to addressing the CDEP is the Variant Allele Frequency Factorization Problem (VAFFP) (El-Kebir et al., 2015).

Given s tumor samples and n mutations identified across these samples, we define a matrix $\boldsymbol{F} \in [0,1]^{s\times n}$, where each element f_{ij} represents the variant VAF value, or equivalently, the fraction of cells that carry mutation j in sample i. The VAFFP seeks to decompose this input matrix $\boldsymbol{F}$ into two matrices: a matrix $\boldsymbol{B} \in \{0,1\}^{n\times n}$ that represents the clonal

[*]These authors contributed equally to this work.

phylogeny, and a matrix $\boldsymbol{U} \in [0,1]^{s \times n}$ that captures the clone proportions in each tumor sample:

$$\boldsymbol{F} = \boldsymbol{U} \cdot \boldsymbol{B} \tag{1}$$

The $\boldsymbol{B}$ matrix is a binary square matrix of size n, where $b_{ij} = 1$ iff clone i contains the mutation j (Gusfield, 1991). The matrix $\boldsymbol{U}$ is an $s \times n$ matrix where u_{ij} is the fraction of clone j in sample i.

The VAFFP operates under two key assumptions: tumors have a monoclonal origin, meaning they arise from a single abnormal cell, and the infinite sites assumption (ISA), which states that mutations occur at most once and cannot disappear over time (Kimura, 1969). Under these assumptions, the tumor's clonal structure can be modeled as a perfect phylogeny (Gusfield, 1991). This model imposes two key constraints: (1) if two clones share a mutation, they must either be identical or ancestrally related, and (2) once a clone acquires a mutation, that mutation is inherited by all its descendants.

Over the years, numerous methods have been developed to solve the CDEP (Sengupta et al., 2014; Yuan et al., 2015; Deshwar et al., 2015; El-Kebir et al., 2015; Malikic et al., 2015; Popic et al., 2015; El-Kebir et al., 2016; Jiang et al., 2016; Husić et al., 2019; Fu et al., 2022; Grigoriadis et al., 2024), with recent advancements addressing reformulations of the problem that incorporate single-cell sequencing-derived information or variants in metastases, and account for temporal resolution (Ross and Markowetz, 2016; El-Kebir et al., 2018; Malikic et al., 2019; Satas et al., 2020; Sollier et al., 2023). These methods primarily focus on reconstructing tumor phylogenies and clonal compositions using both real and simulated data. However, the simulation tools they employ often have limitations. For instance, while MiPUP uses simulated data, it allows only basic parameter adjustments—such as the number of mutations, samples, and reads—and lacks the flexibility to fine-tune biological parameters. BitPhylogeny creates highly realistic and complex simulated datasets representing different modes of evolution, but these simulations are manually crafted and limited in number, posing scalability issues.

Several tools specifically designed for simulating data for the CDEP have also been introduced. Pearsim, written in Python, allows control over parameters like read depth, number of subclones, samples, and mutations (Kulman et al., 2022). OncoLib, a C++ library, facilitates the simulation of tumor heterogeneity and the reconstruction of NGS sequencing data of metastatic tumors, offering control over parameters such as driver mutation probability, per-base sequencing error rate, migration rate, and mutation rate (Qi et al., 2019). Machina, also in C++, provides a framework for simulating metastatic tumors and visualizing their phylogenetic trees and migration graphs (El-Kebir et al., 2018). HeteroGenesis, implemented in Python, simulates heterogeneous tumors at the level of clone genomes, but it is not specifically tailored for CDEP instances and requires additional processing to generate suitable datasets (Tanner et al., 2019).

Visualization of tumor phylogenies is another crucial aspect of studying tumor evolution. Tools like CALDER, Clonevol, SPRUCE, **fishplot**, ClonArch, and **clevRvis** offer solutions for visualizing clonal structures and evolutionary trajectories (Myers et al., 2019; Dang et al., 2017; El-Kebir et al., 2016; Miller et al., 2016; Wu and El-Kebir, 2020; Sandmann et al., 2023). Among these, **fishplot** and **clevRvis** are available as R packages. Additionally, methods for generating consensus trees, such as TuELIP and ConTreeDP, have been developed to summarize multiple phylogenetic trees into a single representative tree (Guang et al., 2023; Fu and Schwartz, 2021).

Despite the availability of existing tools, there remains a lack of options in the R programming environment for realistically simulating tumor evolution in a way that is both flexible and user-friendly, while also enabling effective visualization and comparison.

In this paper, we introduce **GeRnika**, an R package that provides a comprehensive solution for simulating, visualizing, and comparing tumor evolution data. Although **GeRnika**'s data simulation functionality was primarily devised to create instances for solving the CDEP, the simulated data are not restricted to this purpose and can also be used for exploring

evolutionary dynamics in broader contexts. To accommodate diverse research needs, we have implemented the procedures to be highly customizable, allowing users to adjust a wide range of parameters such as the number of clones, selective pressures, mutation rates, and sequencing noise levels. Unlike existing tools that may offer limited customization or are implemented in other programming languages, **GeRnika** is fully integrated into the R environment, making it easy to use alongside other bioinformatics packages. By combining simulation capabilities with visualization and comparison tools in a user-friendly interface, **GeRnika** offers an accessible and flexible option within the R ecosystem for researchers studying tumor evolution. It is important to note that **GeRnika** does not implement algorithms for inferring clonal composition or reconstructing phylogenies from experimental datasets. Instead, it provides a controlled framework for generating, visualizing, and comparing data that can be used to benchmark such methods.

2 Simulation of tumor evolution

The main contribution of this work is the introduction of a novel approach for simulating biologically plausible instances of the VAFFP that accounts for several key factors, including the number of clones, selective pressures, and sequencing noise. In this section, we provide a detailed description of the approach.

Broadly speaking, each problem instance consists of a matrix $\boldsymbol{F}$ containing the VAF values of a set of mutations in a set of samples, as described previously. This matrix is built from a pair of matrices $\boldsymbol{B}$ and $\boldsymbol{U}$ that represent a tumor phylogeny fulfilling the ISA and the proportions of the clones in the samples, respectively, following Equation (1).

In order to simulate the $\boldsymbol{B}$ and $\boldsymbol{U}$ matrices, we have devised two models: a tumor model that simulates the evolutionary history and current state of the tumor, and a sampling model that represents the tumor sampling process. A third model, namely the sequencing noise model, has been devised to optionally introduce sequencing noise to the VAF values in the $\boldsymbol{F}$ matrix, if noisy data is desired. The following subsections describe these models in detail.

2.1 Tumor model

The tumor model generates a clonal tree T and an associated matrix $\boldsymbol{B}$, together with the clone proportions $\boldsymbol{c}$ and tumor blend at the moment of sampling. Briefly, for a tumor with a set of n mutations denoted by M, T is a rooted tree on an n-sized vertex set $V_n = \{v_1, \ldots, v_n\}$, where v_i represents clone i and simultaneously corresponds to the first clone containing mutation M_i. This one-to-one correspondence between clones and mutations allows us to refer to them interchangeably. The tree is further defined by an $(n-1)$-sized edge set E_T, where each edge $e_{ij} \in E_T$ represents a direct ancestral relationship from vertex v_i to vertex v_j.

In our tumor model, T is iteratively generated with a random topology, as follows. First, the root node of T, $\mathcal{R}(T)$, is set, and a random mutation $M_i \in M$ is assigned to it. For each of the remaining $M_j \in M - \{M_i\}$ mutations, a new node v_j is created and the mutation M_j is assigned to this node. The node v_j is then attached as a child to one of the nodes already included in T. To adhere to the ISA model, each newly added node inherits all the mutations present in its parent node.

The attachment of nodes to the tree is not uniformly random. Instead, the nodes in the growing tree T have different probabilities of being selected as parents for the new nodes, depending on the number of ascendants, $\mathcal{A}(v_i)$, they have. Specifically, $\forall v_j \neq \mathcal{R}(T)$, the parent node of v_j is sampled from a multinomial distribution where the probabilities are calculated as:

$$\boldsymbol{p}(v_i; k) = \frac{k^{\frac{|\mathcal{A}(v_i)|+1}{\delta}}}{\sum_{v_l \in V'} k^{\frac{|\mathcal{A}(v_l)|+1}{\delta}}}; \quad v_i \in V' \tag{2}$$

Here, δ represents the depth of the growing tree, i.e., the number of levels or layers in the tree structure. $k \in (0, +\infty)$ is the topology parameter that determines whether the topology tends to be branched, with a decreasing probability for increasing numbers of ascendants ($k < 1$), or linear, with an increasing probability for increasing numbers of ascendants ($k > 1$).

Once T has been generated, it is represented in the form of a $\boldsymbol{B}$ matrix, constructed by initializing an identity matrix B_n and setting b_{ji} to 1 for each pair of nodes v_i and v_j where node v_j is a descendant of node v_i in T.

After obtaining $\boldsymbol{B}$, the proportions of the clones in the whole tumor, denoted as $\boldsymbol{c} = \{c_1, \ldots, c_n\}$, are simulated. It is important to note that these proportions are not the same as those appearing in the $\boldsymbol{U}$ matrix, which represent the *sampled* clone proportions and depend not only on the global clone proportions but also on the spatial distribution of the clones and the sampling sites.

These clone proportions $\boldsymbol{c}$ are calculated by sequentially sampling a Dirichlet distribution at each multifurcation in T, starting from the root. For instance, for a node v_i with children $\mathcal{K}(v_i) = \{v_j, v_k\}$, we draw a sample (x_i, x_j, x_k) that represents the proportions of the parent clone and its two children, respectively, from a Dirichlet distribution $Dir(\alpha_i, \alpha_j, \alpha_k)$. When this sampling is performed at a node $v_i \neq \mathcal{R}(T)$, these proportions are scaled relative to the original proportion of the parent clone. This ensures that the sum rule is met, and that once all multifurcations have been visited, the proportions of all clones in T sum up to one. While several approaches can exist to determine these proportions, this method provides a natural approximation to the problem that can be interpreted as the distribution of the mass or proportion of each clone between itself and its descendants.

The parameters of the Dirichlet distribution depend on the tumor's evolution model. In this work, we consider two fundamental cases: positive selection-driven evolution and neutral evolution. In positive selection-driven evolution, certain mutations confer a growth advantage, while most mutations do not. As a result, the clones carrying these advantageous mutations outcompete other clones and dominate the tumor. Consequently, tumors are predominantly composed of a few dominant clones, with the remaining clones present in too small proportions. Under neutral evolution, instead, there is no significant number of mutations that provide a fitness advantage, and clones accumulate solely due to tumor progression. As a result, all clones are present in similar proportions (Davis et al., 2017).

Based on this, all the parameters for the Dirichlet distribution for positive selection-driven evolution are set to 0.3. For neutral evolution, the parameter corresponding to the parent node (α_p) is set to 5, and the parameters corresponding to the children node(s) (α_c) are set to 10. Different alpha values are used for parent and children nodes in neutral evolution to ensure that clones arising late in the evolution do not end up with proportions that are too small solely due to their position in the topology, preventing the deviation from the expected clone proportion distribution for this type of evolution model. These values have been chosen empirically, and their effect is illustrated in Figure 1, which shows how 5,000 random samples from the mentioned Dirichlet distributions (for the particular case of 3 dimensions, i.e., one parent and two children nodes) are distributed. As observed, in the case of positive selection ($\alpha_i = \alpha_j = \alpha_k = 0.3$), the (x_i, x_j, x_k) values are equally pushed towards the three corners of the simplex. In other words, the samples tend to be sparse, with typically one component having a large value and the rest close to 0. Instead, when neutral selection is adopted ($\boldsymbol{\alpha} = (5, 10, 10)$), the (x_i, x_j, x_k) values concentrate close to the center of the simplex, but with a tendency to deviate towards those components with larger α value. This means that samples (x_i, x_j, x_k) are less sparse in neutral evolution, with larger values for x_2 and x_3 in this case, which represent the children nodes.

Taking into account that marginalizing the Dirichlet distribution results in a Beta distribution, the proportion of the clone $v_i \in V_n \mid v_i \neq \mathcal{R}(T)$ in the tumor, denoted as C_i, follows the distribution:

$$C_i \sim C_{\mathcal{P}(v_i)} \cdot \Gamma_i \cdot \Gamma_i' \tag{3}$$

where

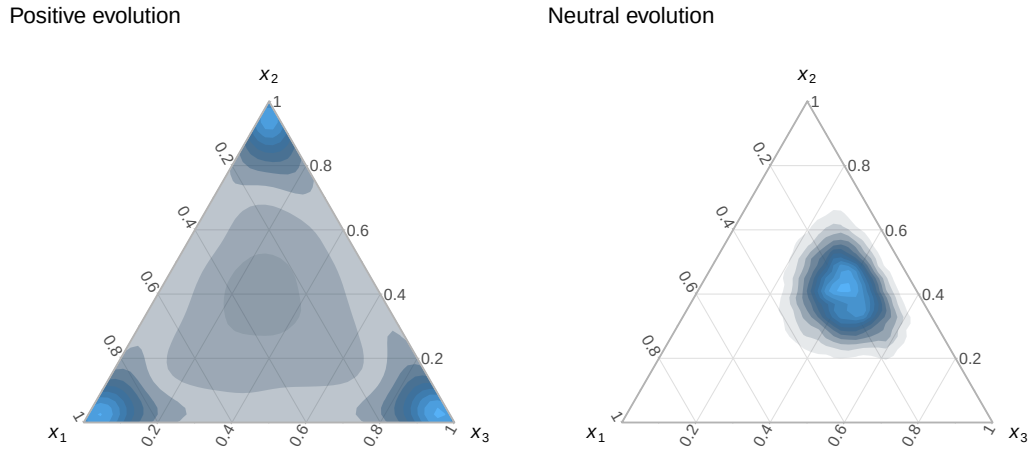

Figure 1: Ternary density plots of 5,000 samples drawn from two 3-dimensional Dirichlet distributions. The parameters of the Dirichlet distribution on the left are $\boldsymbol{\alpha}$ = (0.3, 0.3, 0.3) and the distribution is used to represent positive selection-driven evolution. The distribution on the right has parameters $\boldsymbol{\alpha}$ = (5, 10, 10) and is used to represent neutral evolution. Samples drawn from these distributions (or their generalization to higher spaces) are used to calculate clone proportions in each tree multifurcation.

$$\Gamma_i \sim Beta(\alpha_c, \alpha_p + \alpha_c \cdot (|\mathcal{K}(\mathcal{P}(v_i))| - 1)) \tag{4}$$

and

$$\Gamma'_i = 1 \quad \text{if } |\mathcal{K}(v_i)| = 0 \tag{5}$$

$$\Gamma'_i \sim Beta(\alpha_p, \alpha_c \cdot |\mathcal{K}(v_i)|) \quad \text{if } |\mathcal{K}(v_i)| \neq 0 \tag{6}$$

For the case where $v_i = \mathcal{R}(T)$, the root node, C_i, follows:

$$C_i \sim Beta(\alpha_p, \alpha_c \cdot |\mathcal{K}(v_i)|) \tag{7}$$

Here, α_p and α_c are the parameters of the Dirichlet distribution assigned to parent and child nodes, respectively.

To complete the tumor model, the tumor blend is simulated, which represents the degree of physical mixing between the tumor clones. In order to do this, we simplify the spatial distribution to one dimension and model the tumor as a Gaussian mixture model with n components, where each component G_i represents a tumor clone, and the mixture weights are given by $\boldsymbol{c}$. The variance for all components is set to 1, while the mean values are random variables.

Specifically, we start by selecting a random clone, and its component's mean value is set to 0. Then, the mean values of the remaining $n-1$ components are calculated sequentially by adding d units to the mean value of the previous component. To introduce variability in the tumor blend, the value of d is chosen from the set $\{0, 0.1, \ldots, 4\}$. For $d = 0$, the two clones are completely mixed, while for $d = 4$, they are physically far apart from each other. The choice of the upper limit for d has been determined empirically, considering that with this value, the overlapping area between the two clones becomes negligible.

To ensure the separation between the clones is random and that most of the time the separation is small, we use an exponential-like distribution with the form $Beta(\alpha = 1, \beta = X)$ to sample the values of d. Specifically, we set $\beta = 5$ to ensure that the samples obtained from the mixture are not excessively sparse. We can express this mathematically as:

$$D \sim 4 \cdot Beta(\alpha = 1, \beta = 5) \tag{8}$$

2.2 Sampling simulation

So far, we have described how the clones of a tumor are modelled by the tumor model. However, in real practice, there is no easy way of observing these global properties of a tumor. Instead, we typically have access to information provided by samples or biopsies. This means that certain tumor characteristics, such as the real clone proportions $\boldsymbol{c}$, cannot be directly obtained. Instead, we can only determine the *sampled* clone proportions, which depend on the specific sampling procedure employed. Unless there is a perfectly uniform mixture of the clone cells, their sampled proportions will not match the global proportions. These sampled clone proportions are, in fact, the $\boldsymbol{u}_i$. elements in the $\boldsymbol{U}$ matrix.

The sampling simulation we have devised simulates the physical sampling of the tumor and allows us to construct the $\boldsymbol{U}$ matrix of the problem. This procedure operates on the data simulated using the tumor model. Specifically, it simulates a sampling procedure carried out in a grid manner over the tumor Gaussian mixture model described in the previous section. Let G_1 and G_n be the components with the lowest and largest mean values, respectively, in the Gaussian mixture model. The 1st and m^{th} sampling points in the grid are always set to $\mu_{G_1} - 2.8 \cdot \sigma_{G_1}$ and $\mu_{G_n} + 2.8 \cdot \sigma_{G_n}$, respectively, and the remaining m-2 sampling points are determined by dividing the range between these two endpoints into $m - 1$ equal intervals.

The densities of the Gaussian distributions at each sampling point are multiplied by the global proportion of the clones sampled from the Dirichlet distributions, so that for each sampling point i, the fraction of clone j, p_{ij}, is proportional to their product:

$$p_{ij} \propto c_j \cdot \phi_{ij} \tag{9}$$

where c_j is the global proportion of clone j and ϕ_{ij} is the density of the Gaussian component associated with clone j at sampling point i.

Finally, to account for the effect of cell count in the samples, a multinomial distribution is used to sample a given number of cells n_c for each tumor sample. In that distribution, the probability of selecting each clone at sampling site i is given by $(p_{i1}, \ldots, p_{in})$. The resulting values determine the final tumor clone composition in sample i, which are represented in the matrix $\boldsymbol{U}$:

$$U_{i.} \sim \frac{M(n = n_c, p = (p_{i1}, \ldots, p_{in}))}{100} \tag{10}$$

Note that selecting a relatively low value for n in the multinomial distribution can lead to clones with very low frequencies being modeled as absent in the sample, with composition values equal to 0. This is indeed more realistic than truly observing them with such low frequencies.

2.3 Sequencing noise simulation

Up to this point, the $\boldsymbol{B}$ and $\boldsymbol{U}$ matrices of an instance have been simulated. In case we are simulating noise-free data, the simulation is complete once Equation (1) is applied to obtain the $\boldsymbol{F}$ matrix.

As a brief reminder, each element f_{ij} in $\boldsymbol{F}$ denotes the frequency or VAF of the mutation M_j in sample i or, in other words, the proportion of sequencing reads that carry the mutation M_j in that particular sample. This also means that the proportion of reads in that sample that do not observe the mutation but instead contain the reference nucleotide is 1 - f_{ij}.

However, empirical factors can artificially alter the VAF value, leading it to deviate from the true ratio between the variant and total allele molecule counts. One of these factors is the noise introduced during the DNA sequencing process itself, which can arise in two

main ways. First, limitations of the sequencing instrument can lead to incorrect nucleotide readings of DNA fragments. For example, a position that actually contains nucleotide A may be read as a T. Second, there can be a biased number of reads produced for a particular site, which can result from chemical reaction peculiarities or simply because not all fragments are sequenced. These limitations can, however, be mitigated to some extent. For instance, it has been shown that a high depth of coverage, which refers to the average number of reads that cover each position, can lead to more accurate VAF values (Petrackova et al., 2019).

In order to incorporate the effect of sequencing noise in the data instances, we have developed a procedure to simulate sequencing noise. This procedure introduces noise to the $\boldsymbol{F}$ matrix and generates a noisy matrix $\boldsymbol{F^{(n)}}$, where $\boldsymbol{F^{(n)}} \neq \boldsymbol{U} \cdot \boldsymbol{B}$. The procedure simulates noise at the level of the sequencing reads and recalculates the new $f_{ij}^{(n)}$ values, as follows.

The sequencing depth r at the genomic position where M_j occurs in sample i is distributed according to a negative binomial distribution:

$$r_{ij} \sim NB(\mu = \mu_{sd}, \alpha = 5) \tag{11}$$

where μ_{sd} represents the mean sequencing depth, which is the average number of reads covering the genomic position of mutation M_j in the sample, and α is the dispersion parameter, which controls the variability of the sequencing depth around the mean and is fixed at 5.

The number of reads supporting the alternate allele r_{ij}^{a} is then modeled by a binomial distribution:

$$r_{ij}^{a} \sim B(n = r_{ij}, p = f_{ij}) \tag{12}$$

In sequencing data, errors can occur due to limitations inherent to the sequencing methodology. These errors vary depending on the technology used.

To simulate the effect of these errors on the VAF values, the number of reads $r_{ij}^{a\prime}$ that, despite originally supporting the alternate allele, contain a different allele as a result of a sequencing error, is modeled using a binomial distribution:

$$r_{ij}^{a\prime} \sim B(n = r_{ij}^{a}, p = \varepsilon), \tag{13}$$

where ε represents the sequencing error rate.

We also need to consider the situation where the reads contain the reference nucleotide but are read with the alternate allele as a result of this error. This can be better understood with an example. Let's imagine that at a certain genomic position, the normal cells have a T, but in some cells, there is a mutation where the T has changed to an A. In this case, for the normal cells, with a rate of ε, a sequencing error may occur, resulting in a read of C, G, or A instead of T, each with an equal chance. Therefore, in approximately $\frac{\varepsilon}{3}$ of the cases, reads with the mutation of interest will arise from normal reads:

$$r_{ij}^{r\prime} \sim B(n = r_{ij} - r_{ij}^{a}, p = \frac{\varepsilon}{3}) \tag{14}$$

Thus, taking all these into consideration, the final noisy VAF values $f_{ij}^{(n)}$ are simulated as:

$$f_{ij}^{(n)} = \frac{r_{ij}^{a} - r_{ij}^{a\prime} + r_{ij}^{r\prime}}{r_{ij}} \tag{15}$$

By default, the sequencing error rate ε is set to 0.001, following commonly reported values for Illumina data (Loman et al., 2012).

As an illustration of the effect of the noise model, in Figure 2, we have depicted the density of the mean absolute error between the $\boldsymbol{F^{(n)}}$ matrix and its corresponding noise-free

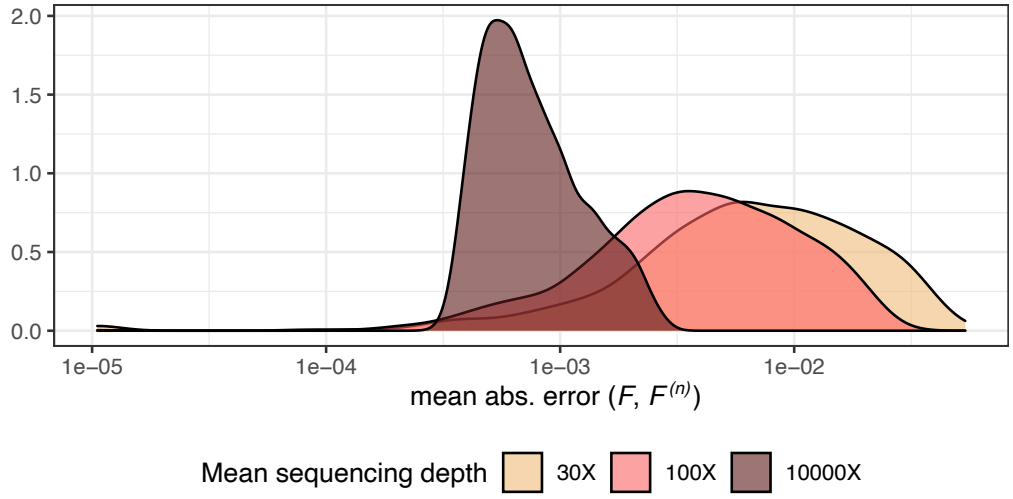

Figure 2: Density of the mean absolute error in noisy $\boldsymbol{F}$ matrices for different μ_{sd} values that correspond to different noise levels.

$\boldsymbol{F}$ matrix for a collection of noisy instances. As can be seen, as μ_{sd} increases, the error introduced to the $\boldsymbol{F}^{(n)}$ matrix decreases. This is expected because the r^a_{ij} values follow a binomial distribution as described in Equation (12), where the number of trials is determined by μ_{sd} as shown in Equation (11), and the event probability corresponds to the $f^{(n)}_{ij}$ value. Therefore, the larger the number of trials, the closer the noisy VAF value is to the noise-free VAF value.

As a final remark, it is important to note that although our data simulation procedure follows the ISA, the addition of noise may cause the resulting data to break this assumption.

3 The package

GeRnika provides three main functionalities for studying tumor evolution data: (I) simulating artificial tumor evolution, (II) visualizing tumor phylogenies, and (III) comparing tumor phylogenies. This section explains the functions that support these features. Additionally, we describe extra data provided by **GeRnika** that users can use to try the methods in the package.

3.1 Simulation methods

To enable users to simulate tumor evolution data, **GeRnika** provides various functions inspired by the methods described in section 2.2. GeRnika offers two options: a single method for streamlined simulations and separate methods for performing each step individually, allowing users to customize or replace specific parts of the process.

create_instance

The main function for streamlined tumor data simulation is `create_instance`. This function provides a convenient way to perform the entire simulation process in a single step. The following command demonstrates how to use it to generate the artificial data:

```
create_instance(n, m, k, selection, noisy = TRUE, depth = 30, seed = Sys.time())
```

where each argument of the method is described as follows:

- `n`: An integer representing the number of clones.

- `m`: An integer representing the number of samples.
- `k`: A numeric value that determines the linearity of the tree topology. Also referred to as the topology parameter. Increasing values of this parameter increase the linearity of the topology. When `k` is set to 1, all nodes have equal probabilities of being chosen as parents, resulting in a uniformly random topology.
- `selection`: A character string representing the evolutionary mode the tumor follows. This should be either "positive" or "neutral".
- `noisy`: A logical value (`TRUE` by default) indicating whether to add noise to the frequency matrix. If `TRUE`, noise is added to the frequency matrix. If `FALSE`, no noise is added.
- `depth`: A numeric value (30 by default) representing the mean depth of sequencing.
- `seed`: A numeric value (`Sys.time()` by default) used to set the seed for the random number generator.

The `create_instance` function returns a list containing the following components:

- `F_noisy`: A matrix representing the noisy frequencies of each mutation across samples. If the `noisy` parameter is set to `FALSE`, this matrix is equal to `F_true`.
- `B`: A matrix representing the relationships between mutations and clones in the tumor.
- `U`: A matrix representing the frequencies of the clones across the set of samples.
- `F_true`: A matrix representing the noise-free frequencies of each mutation across the samples.

As explained, the `create_instance` function generates all matrices representing frequencies, proportions, and the phylogeny of the simulated tumor data in a single step. However, **GeRnika** also provides individual functions for simulating each of these elements independently, providing users with greater control over the characteristics of the simulated tumor data.

create_B, create_U, create_F and add_noise

These methods provide specialized functions to generate each matrix involved in representing tumor evolution data. These functions include the following:

- `create_B`: This function generates a mutation matrix ($\boldsymbol{B}$ matrix) for a tumor phylogenetic tree with a given number of nodes and a value `k` determining the linearity of the tree topology.
- `create_U`: This function calculates the $\boldsymbol{U}$ matrix, containing the frequencies of each clone in a set of samples, based on a $\boldsymbol{B}$ matrix, the number of samples considered, the number of cells in each sample, and the evolutionary mode of the tumor.
- `create_F`: This function generates the $\boldsymbol{F}$ matrix, which contains mutation frequency values for a series of mutations across a collection of tumor biopsies or samples. The matrix is computed based on a pair of matrices, $\boldsymbol{U}$ and $\boldsymbol{B}$, and considers whether the mutations are heterozygous.
- `add_noise`: This function introduces sequencing noise into the noise-free $\boldsymbol{F}$ matrix generated by the `create_F` method. Users can specify the mean sequencing depth and the overdispersion parameter, which are used to simulate sequencing depth based on a negative binomial distribution.

The reader is encouraged to refer to the package documentation for more information about these functions and their parameters.

3.2 Visualization methods

The following functions enable the visualization of tumor evolution data by generating phylogenetic trees based on the data under analysis.

Phylotree S4 class

To simplify the execution of its functionalities, **GeRnika** utilizes the `"Phylotree"` class. The `"Phylotree"` S4 class is a data structure specifically designed to represent phylogenetic trees, facilitating the use of the package's methods and ensuring their computational efficiency. The attributes of the `"Phylotree"` class are as follows:

- `B`: A data.frame containing the square matrix that represents the ancestral relationships among the clones in the phylogenetic tree (***B*** matrix).
- `clones`: A vector representing the indices of the clones in the ***B*** matrix.
- `genes`: A vector indicating the index of the gene that firstly mutated in each clone within the ***B*** matrix.
- `parents`: A vector indicating the parent clones for each clone in the phylogenetic tree.
- `tree`: A `"Node"` class object representing the phylogenetic tree (this class is inherited from the **data.tree** package).
- `labels`: A vector containing the gene tags associated with the nodes in the phylogenetic tree.

A customized `"Phylotree"` class object can be instantiated with custom attributes using the `create_instance` method. This method takes all the attributes according to the `"Phylotree"` class as arguments. Alternatively, **GeRnika** provides a function that automatically generates a `"Phylotree"` class object on the basis of a given ***B***.

B_to_phylotree

In order to instantiate an object of the "`Phylotree`" class, the following command can be used:

```
B_to_phylotree(B, labels = NA)
```

where each argument of the method is described as follows:

- `B`: A square ***B*** matrix that represents the phylogenetic tree.
- `labels`: An optional vector containing the tags of the genes in the phylogenetic tree. `NA` by default.

This function returns an object of the `"Phylotree"` class, automatically generating its attributes based on `B`, which represents the phylogenetic tree of the tumor under analysis.

Once instantiated, the phylogenetic tree in a `"Phylotree"` class object can be visualized using the generic `plot` function, which takes the `"Phylotree"` object as its argument. The `plot` function also includes a `labels` argument that can be set to `TRUE` to display node labels on the phylogenetic tree, using the gene tags stored within the `"Phylotree"` object.

The **GeRnika** package provides the `plot_proportions` function for visualizing phylogenetic trees, with node sizes and colors reflecting the proportions of each clone. This function requires two inputs: a `"Phylotree"` class object representing the phylogenetic tree and a numeric vector or matrix specifying clone proportions. If a vector is provided, a single tree is plotted, with the node sizes and colors determined by the values in the vector. Instead, if

a matrix is provided, such as the $\boldsymbol{U}$ matrix that represents the frequencies of clones across samples, the function plots one tree for each row of the matrix. Each tree is generated based on the clone proportions specified in the corresponding row. Additionally, users can enable node labeling by setting the `labels` argument to `TRUE`, which annotates the tree nodes with gene tags from the `"Phylotree"` object.

3.3 Comparison methods

This section describes the methods included in **GeRnika** that facilitate the comparison of tumor phylogenies.

A fundamental approach for comparing two phylogenetic trees is to determine if their evolutionary histories are equivalent. The `equals` function performs this comparison by accepting two `"Phylotree"` class objects as arguments. This function returns a boolean value indicating whether the provided phylogenetic trees are equivalent.

To analyze similarities and differences between two phylogenetic trees, the `find_common_subtrees` function identifies and plots all maximal common subtrees between them. In addition to visualizing these subtrees, the function outputs the number of shared and unique edges (those present in only one of the trees) and calculates the distance between the trees, defined as the sum of their unique edges. This method also includes an option to label the maximal common subtrees with gene tags by setting `labels = TRUE`.

The `combine_trees` function generates a *consensus tree* by combining the nodes and edges of two `"Phylotree"` class objects. The consensus tree highlights the nodes and edges that form common subtrees between the original trees, as well as the independent edges unique to each tree, which are displayed with reduced opacity. This method also allows labeling the nodes with gene tags by setting `labels = TRUE` and customizing the colors of the consensus tree by passing a 3-element hexadecimal vector to the `palette` argument.

3.4 Exported data

GeRnika provides various exported data instances to help users easily explore the package's functionalities. These are as follows:

- `B_mats`: A list of 10 trios of $\boldsymbol{B}$ matrices. Each trio includes a real $\boldsymbol{B}$ matrix and two $\boldsymbol{B}$ matrices generated using different algorithms that infer evolutionary relationships from a given $\boldsymbol{F}$ matrix. These matrices serve as illustrative examples for testing and exploring the package's functionalities.
- `palettes`: A data frame containing three predefined palettes for use with methods in **GeRnika** that require color palettes.

4 Examples

In this section we show examples of the use of the methods explained in section 2.3. Please note that in the following examples, we will set the seeds of non-deterministic methods to a predefined value to ensure reproducibility.

4.1 Simulating tumor evolution data

The simulation of tumor clonal data involves generating the matrices $\boldsymbol{B}$, $\boldsymbol{U}$, $\boldsymbol{F}$, and $\boldsymbol{F}^{(n)}$ associated with a specific instance. For example, we can simulate a noisy instance of a tumor composed of 5 clones/mutations, which has evolved under neutral evolution with a k value of 0.5, and from which 3 samples have been taken in a single line of code, as follows:

```
> I <- create_instance(n = 5, m = 3, k = 0.5, selection = "neutral", seed = 1)
```

```
> I

$F_noisy
         mut1       mut2      mut3      mut4      mut5
sample1 1.000 0.09090909 0.0000000 0.2777778 0.3548387
sample2 1.000 0.20000000 0.2631579 0.8536585 0.2000000
sample3 0.975 0.03846154 1.0000000 1.0000000 0.0000000

$B
       mut1 mut2 mut3 mut4 mut5
clone1    1    0    0    0    0
clone2    1    1    0    1    0
clone3    1    0    1    1    0
clone4    1    0    0    1    0
clone5    1    0    0    1    1

$U
        clone1 clone2 clone3 clone4 clone5
sample1   0.59   0.13   0.00   0.01   0.27
sample2   0.13   0.27   0.24   0.19   0.17
sample3   0.00   0.04   0.89   0.07   0.00

$F_true
        mut1 mut2 mut3 mut4 mut5
sample1    1 0.13 0.00 0.41 0.27
sample2    1 0.27 0.24 0.87 0.17
sample3    1 0.04 0.89 1.00 0.00
```

Using this approach, the previously mentioned four matrices are simulated. Note that the noise-free $\boldsymbol{F}$ matrix is referred to as `F_true` in the package's code, while the noisy $\boldsymbol{F}^{(n)}$ is denoted as `F_noisy`.

The previous method allows users to generate instances easily and quickly. However, some users may require more precise control over the data, which can be achieved using the `create_B`, `create_U`, `create_F`, and `add_noise` methods. For examples on how to use these methods, please refer to the package documentation.

4.2 Visualizing tumor phylogenies

Once the matrices associated with our tumor instance have been generated, we can create a `"Phylotree"` class object, as follows:

```
> phylotree <- B_to_phylotree(B = I$B)
> phylotree

An object of class "Phylotree"
Slot "B":
       mut1 mut2 mut3 mut4 mut5
clone1    1    0    0    0    0
clone2    1    1    0    1    0
clone3    1    0    1    1    0
clone4    1    0    0    1    0
clone5    1    0    0    1    1

Slot "clones":
mut1 mut2 mut3 mut4 mut5
```

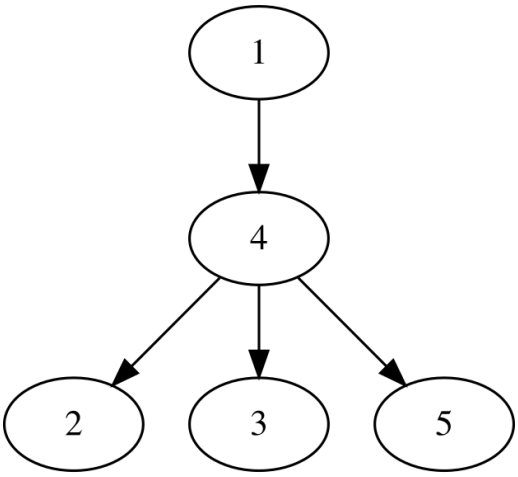

Figure 3: Phylogenetic tree associated to the generated "Phylotree" class object.

```
   1    2    3    4    5

Slot "genes":
mut1 mut2 mut3 mut4 mut5
   1    2    3    4    5

Slot "parents":
[1] -1  4  4  1  4

Slot "tree":
  levelName
1 1
2  °--4
3      ¦--2
4      ¦--3
5      °--5

Slot "labels":
[1] "mut1" "mut4" "mut2" "mut3" "mut5"
```

Since no list of tags is provided to the `labels` parameter, a default set of labels is automatically assigned to the instantiated "Phylotree" class object.

Afterwards, we can visualize the tumor phylogeny associated to the simulated $\boldsymbol{B}$ matrix by using the generic `plot` method, as follows:

```
> plot(phylotree)
```

The resulting plot is shown in Figure 3. Instead of clone numbers, the user can utilize the predefined tags in the "Phylotree" class object to label the nodes in the tree by setting the `labels = TRUE` parameter in the `plot` function.

When plotting a "Phylotree" class object, its nodes can be resized according to the proportions of the clones that compose the tumor samples. To achieve this, we can use the $\boldsymbol{U}$ matrix from the previously generated instance to determine the proportions of the clones, as shown below:

```
> plot_proportions(phylotree, I$U, labels = TRUE)
```

The resulting plot is shown in Figure 4. This method plots the proportions of the $\boldsymbol{U}$ matrix, where each tree represents a sample from the $\boldsymbol{U}$ matrix, illustrating the proportion

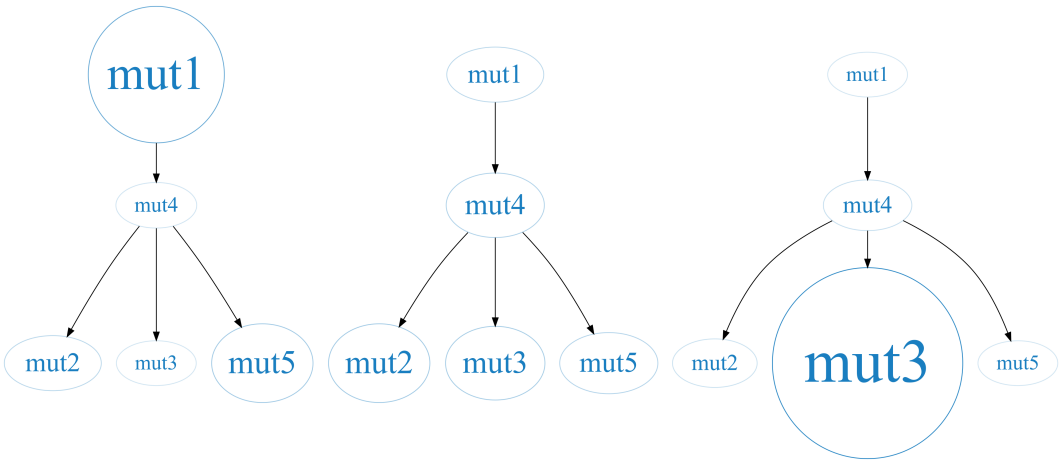

Figure 4: Phylogenetic trees associated to the generated "Phylotree" class object, using the proportions associated to the previously generated $\boldsymbol{U}$ matrix.

of each clone within that specific sample. In this case, we have set the `labels` parameter to `TRUE` to label the nodes in the tree using the predefined tags "mut1", "mut4", "mut2", "mut3", and "mut5".

4.3 Comparing tumor phylogenies

Now, we present examples showing the use of **GeRnika**'s functionalities for comparing tumor phylogenies. For this purpose, we will use the `B_mats` object included in the **GeRnika** package, which contains 10 $\boldsymbol{B}$ matrix trios. Specifically, we will use the first trio of matrices, and set a predefined set of tags for the clones in the trees:

```
> B_mats <- GeRnika::B_mats

> B_real <- B_mats[[1]]$B_real
> B_alg1 <- B_mats[[1]]$B_alg1
> B_alg2 <- B_mats[[1]]$B_alg2

> tags <- c("TP53", "KRAS", "PIK3CA", "APC", "EGFR", "BRCA1", "PTEN", "BRAF",
            "MYC", "CDKN2A")

> phylotree_real <- B_to_phylotree(B = B_real, labels = tags)
> phylotree_alg2 <- B_to_phylotree(B = B_alg2, labels = tags)
> phylotree_alg1 <- B_to_phylotree(B = B_alg1, labels = tags)

> plot(phylotree_real, labels=TRUE)
> plot(phylotree_alg1, labels=TRUE)
> plot(phylotree_alg2, labels=TRUE)
```

The plots of the three instantiated `Phylotree` class objects are depicted in Figure 5.

We can check if the phylogenies of two tumors are equivalent using the `equals` method:

```
> equals(phylotree_1 = phylotree_real, phylotree_2 = phylotree_alg1)
[1] FALSE

> equals(phylotree_1 = phylotree_real, phylotree_2 = phylotree_real)
[1] TRUE
```

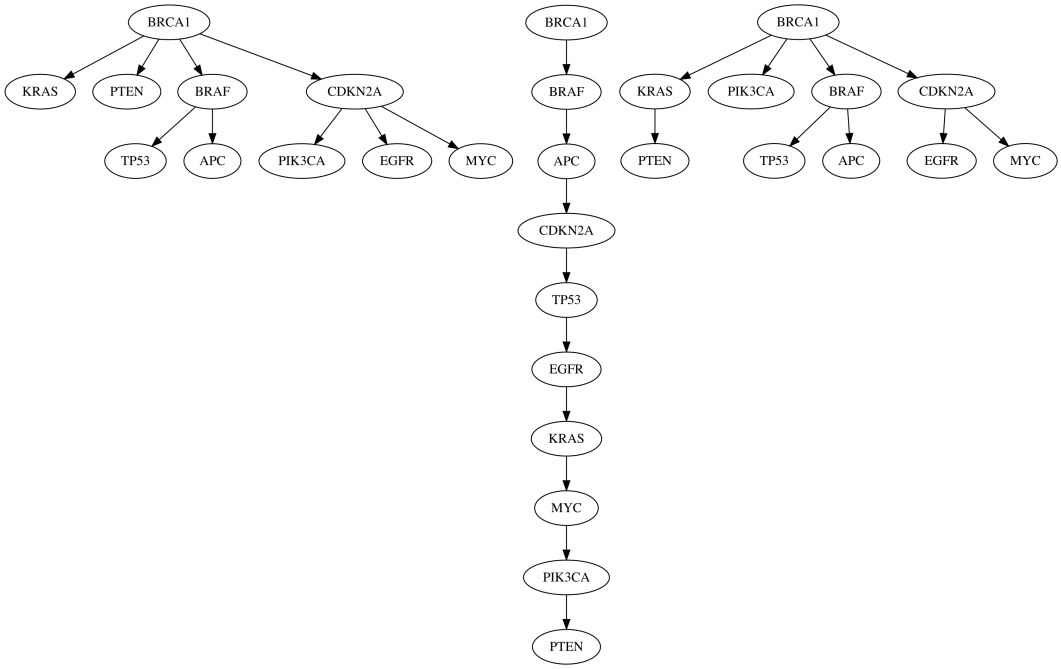

Figure 5: `phylotree_real`, `phylotree_alg2` and `phylotree_alg1`, from the left to the right.

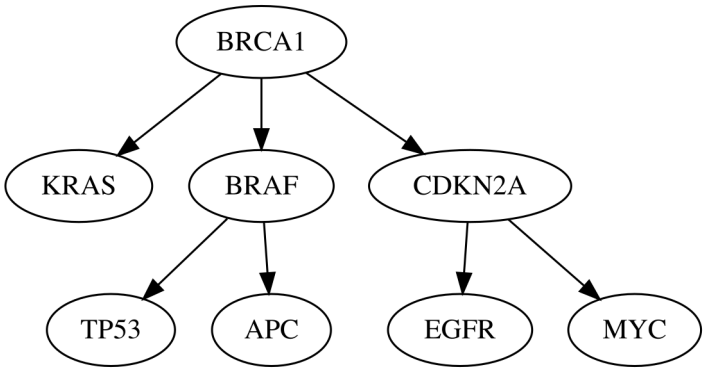

Figure 6: Maximal common subtrees between `phylotree_real` and `phylotree_alg2` using predefined tags. In this case, there exists a single common subtree, but there may exist more in other cases.

In this case, `phylotree_real` and `phylotree_alg1` are not identical, as some edges present in `phylotree_real` are absent in `phylotree_alg1`, and vice versa. However, a phylogenetic tree will always be identical to itself, as shown when comparing `phylotree_real` to itself.

To find the maximal common subtrees between two phylogenetic trees, we do it using the following command:

```
> find_common_subtrees(phylotree_1 = phylotree_real, phylotree_2 = phylotree_alg2,
                       labels = TRUE)

Independent edges of tree1: 2

Independent edges of tree2: 2

Common edges: 7

Distance: 4
```

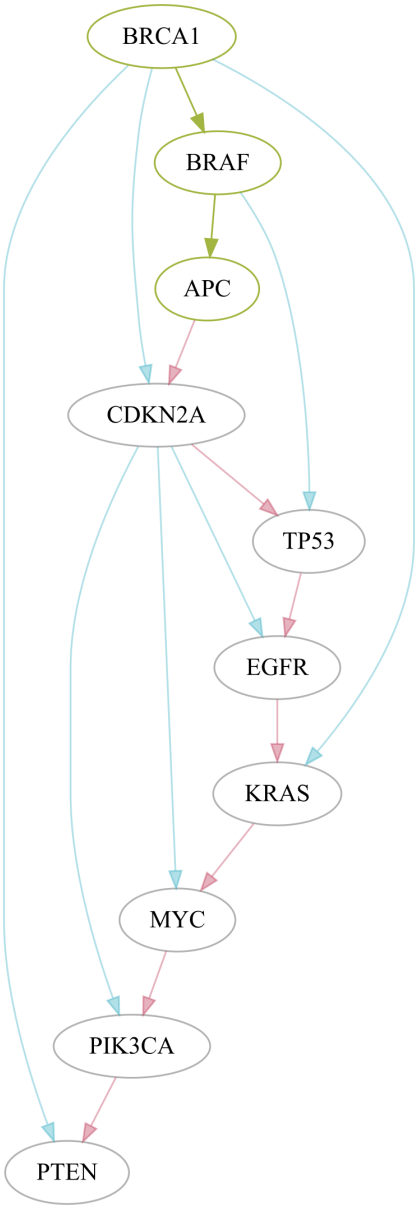

Figure 7: Consensus tree between `phylotree_real` and `phylotree_alg1` using the *Lancet* palette and predefined tags.

The maximal common subtrees (in this case, one subtree) between `phylotree_real` and `phylotree_alg2` are shown in Figure 6. Note that the clones in the maximal common subtree are represented by the predefined tags in the `Phylotree` class objects as we have set `labels = TRUE`. Additionally, this method prints the number of common and independent edges of the trees, along with the distance between them.

Finally, we generate the consensus tree between two phylogenetic trees using one of the custom palettes offered by **GeRnika**, specifically the *Lancet* palette, and the predefined tags for the clones as follows:

```
> palette <- GeRnika::palettes$Lancet

> consensus_real_alg1 <- combine_trees(phylotree_1 = phylotree_real,
                                       phylotree_2 = phylotree_alg1,
                                       labels = TRUE,
                                       palette = palette)
```

```
> DiagrammeR::render_graph(consensus_real_alg1)
```

The consensus tree between `phylotree_real` and `phylotree_alg1` is depicted in Figure 7. Here, the nodes and the edges that compose the common subtrees between the original trees are green. In addition, pink edges denote the independent edges of the tree passed as the first parameter of the method, while blue edges represent the independent edges of the second tree. Note that the independent edges of both trees are presented with translucent colors.

5 Conclusions

GeRnika is a comprehensive R package designed to address a critical gap in the tools available for studying tumor evolution within the R environment. To this end, it provides researchers with an integrated suite for simulating, visualizing, and comparing tumor phylogenies. Unlike many existing tools, **GeRnika** is fully implemented in R, making it particularly accessible for the bioinformatics community, which widely relies on R for data analysis and visualization.

One of **GeRnika**'s key contributions is providing tools to generate biologically plausible datasets for studying intratumoral heterogeneity and clonal dynamics. With varied, easily customizable parameters—controlling features such as clonal tree topology, selective pressures, and sequencing noise—**GeRnika** enables exploration of a wide range of evolutionary patterns and complexities that provide a valuable resource for testing new methods and hypotheses in tumor heterogeneity research.

Beyond its core simulation features, **GeRnika** includes tools for visualizing and comparing tumor phylogenies, offering a unified solution that eliminates the need for multiple packages or complex data processing workflows. Future work will focus on enhancing **GeRnika**'s compatibility with other R packages related to tumor evolution, allowing for easier integration with existing resources.

Overall, **GeRnika** provides an accessible, user-friendly tool that supports research into intratumoral heterogeneity, with the potential to substantially advance tumor phylogeny research. While it does not perform clonal deconvolution or phylogeny inference from real sequencing data, **GeRnika** serves as a valuable platform for simulation, visualization, and benchmarking, supporting the development and evaluation of such algorithms.

6 R software

The R package **GeRnika** is now available on CRAN.

References

R. Burrell, N. Mcgranahan, J. Bartek, and C. Swanton. The causes and consequences of genetic heterogeneity in cancer evolution. *Nature*, 501:338–45, 09 2013. doi: 10.1038/nature12625. [p1]

H. Dang, B. White, S. Foltz, C. Miller, J. Luo, R. Fields, and C. Maher. ClonEvol: clonal ordering and visualization in cancer sequencing. *Annals of Oncology*, 28(12):3076–3082, 2017. doi: 10.1093/annonc/mdx517. [p2]

A. Davis, R. Gao, and N. Navin. Tumor evolution: Linear, branching, neutral or punctuated? *Biochimica et Biophysica Acta (BBA)-Reviews on Cancer*, 1867(2):151–161, 2017. doi: 10.1016/j.bbcan.2017.01.003. [p4]

A. G. Deshwar, S. Vembu, C. K. Yung, G. H. Jang, L. Stein, and Q. Morris. PhyloWGS: reconstructing subclonal composition and evolution from whole-genome sequencing of tumors. *Genome Biology*, 16(1):1–20, 2015. doi: 10.1186/s13059-015-0602-8. [p2]

M. El-Kebir, L. Oesper, H. Acheson-Field, and B. J. Raphael. Reconstruction of clonal trees and tumor composition from multi-sample sequencing data. *Bioinformatics*, 31(12):62–70, 06 2015. ISSN 1367-4803. doi: 10.1093/bioinformatics/btv261. [p1, 2]

M. El-Kebir, G. Satas, L. Oesper, and B. J. Raphael. Inferring the mutational history of a tumor using multi-state perfect phylogeny mixtures. *Cell Systems*, 3(1):43–53, 2016. doi: 10.1016/j.cels.2016.07.004. [p2]

M. El-Kebir, G. Satas, and B. J. Raphael. Inferring parsimonious migration histories for metastatic cancers. *Nature Genetics*, 50(5):718–726, 2018. doi: 10.1038/s41588-018-0106-z. [p2]

X. Fu and R. Schwartz. ConTreeDP: A consensus method of tumor trees based on maximum directed partition support problem. In *2021 IEEE International Conference on Bioinformatics and Biomedicine (BIBM)*, pages 125–130. IEEE, 2021. doi: 10.1101/2021.10.13.463978. [p2]

X. Fu, H. Lei, Y. Tao, and R. Schwartz. Reconstructing tumor clonal lineage trees incorporating single-nucleotide variants, copy number alterations and structural variations. *Bioinformatics*, 38(Supplement_1):i125–i133, 2022. doi: 10.1093/bioinformatics/btac253. [p2]

K. Grigoriadis, A. Huebner, A. Bunkum, E. Colliver, A. M. Frankell, M. S. Hill, K. Thol, N. J. Birkbak, C. Swanton, S. Zaccaria, et al. CONIPHER: a computational framework for scalable phylogenetic reconstruction with error correction. *Nature Protocols*, 19(1):159–183, 2024. doi: 10.1038/s41596-023-00913-9. [p2]

Z. Guang, M. Smith-Erb, and L. Oesper. A weighted distance-based approach for deriving consensus tumor evolutionary trees. *Bioinformatics*, 39(Supplement_1):i204–i212, 2023. doi: 10.1093/bioinformatics/btad230. [p2]

D. Gusfield. Efficient algorithms for inferring evolutionary trees. *Networks*, 21(1):19–28, 1991. doi: 10.1002/net.3230210104. [p2]

E. Husić, X. Li, A. Hujdurović, M. Mehine, R. Rizzi, V. Mäkinen, M. Milanič, and A. I. Tomescu. MIPUP: minimum perfect unmixed phylogenies for multi-sampled tumors via branchings and ILP. *Bioinformatics*, 35(5):769–777, 2019. doi: 10.1093/bioinformatics/bty683. [p2]

Y. Jiang, Y. Qiu, A. J. Minn, and N. R. Zhang. Assessing intratumor heterogeneity and tracking longitudinal and spatial clonal evolutionary history by next-generation sequencing. *Proceedings of the National Academy of Sciences*, 113(37):E5528–E5537, 2016. doi: 10.1073/pnas.1522203113. [p2]

M. Kimura. The number of heterozygous nucleotide sites maintained in a finite population due to steady flux of mutations. *Genetics*, 61(4):893, 1969. doi: 10.1093/genetics/61.4.893. [p2]

E. Kulman, J. Wintersinger, and Q. Morris. Reconstructing cancer phylogenies using Pairtree, a clone tree reconstruction algorithm. *STAR Protocols*, 3(4):101706, 2022. doi: 10.1016/j.xpro.2022.101706. [p2]

N. J. Loman, R. V. Misra, T. J. Dallman, C. Constantinidou, S. E. Gharbia, J. Wain, and M. J. Pallen. Performance comparison of benchtop high-throughput sequencing platforms. *Nature Biotechnology*, 30(5):434–439, 2012. doi: 10.1038/nbt.2198. [p7]

S. Malikic, A. W. McPherson, N. Donmez, and C. S. Sahinalp. Clonality inference in multiple tumor samples using phylogeny. *Bioinformatics*, 31(9):1349–1356, 2015. doi: 10.1093/bioinformatics/btv003. [p2]

S. Malikic, F. R. Mehrabadi, S. Ciccolella, M. K. Rahman, C. Ricketts, E. Haghshenas, D. Seidman, F. Hach, I. Hajirasouliha, and S. C. Sahinalp. PhISCS: a combinatorial approach for subperfect tumor phylogeny reconstruction via integrative use of single-cell and bulk sequencing data. *Genome research*, 29(11):1860–1877, 2019. doi: 10.1101/gr.234435.118. [p2]

F. Marass, F. Mouliere, K. Yuan, N. Rosenfeld, and F. Markowetz. A phylogenetic latent feature model for clonal deconvolution. *The Annals of Applied Statistics*, 10:2377–2404, 2016. doi: 10.1214/16-AOAS986. [p1]

C. A. Miller, J. McMichael, H. X. Dang, C. A. Maher, L. Ding, T. J. Ley, E. R. Mardis, and R. K. Wilson. Visualizing tumor evolution with the fishplot package for R. *BMC Genomics*, 17: 1–3, 2016. doi: 10.1186/s12864-016-3195-z. [p2]

M. A. Myers, G. Satas, and B. J. Raphael. CALDER: Inferring phylogenetic trees from longitudinal tumor samples. *Cell Systems*, 8(6):514–522, 2019. doi: 10.1016/j.cels.2019.05.010. [p2]

P. C. Nowell. The clonal evolution of tumor cell populations. *Science*, 194(4260):23–28, 1976. doi: 10.1126/science.959840. [p1]

A. Petrackova, M. Vasinek, L. Sedlarikova, T. Dyskova, P. Schneiderova, T. Novosad, T. Papajik, and E. Kriegova. Standardization of sequencing coverage depth in NGS: recommendation for detection of clonal and subclonal mutations in cancer diagnostics. *Frontiers in Oncology*, 9:851, 2019. doi: 10.3389/fonc.2019.00851. [p7]

V. Popic, R. Salari, I. Hajirasouliha, D. Kashef-Haghighi, R. B. West, and S. Batzoglou. Fast and scalable inference of multi-sample cancer lineages. *Genome Biology*, 16(1):91, 2015. doi: 10.1186/s13059-015-0647-8. [p2]

Y. Qi, Y. Luo, and M. El-Kebir. OncoLib. https://github.com/elkebir-group/OncoLib/, 2019. URL https://github.com/elkebir-group/OncoLib/. [p2]

E. M. Ross and F. Markowetz. OncoNEM: inferring tumor evolution from single-cell sequencing data. *Genome biology*, 17:1–14, 2016. doi: 10.1186/s13059-016-0929-9. [p2]

S. Sandmann, C. Inserte, and J. Varghese. clevRvis: visualization techniques for clonal evolution. *GigaScience*, 12:giad020, 2023. doi: 10.1093/gigascience/giad020. [p2]

G. Satas, S. Zaccaria, G. Mon, and B. J. Raphael. SCARLET: single-cell tumor phylogeny inference with copy-number constrained mutation losses. *Cell systems*, 10(4):323–332, 2020. doi: 10.1016/j.cels.2020.04.001. [p2]

S. Sengupta, J. Wang, J. Lee, P. Müller, K. Gulukota, A. Banerjee, and Y. Ji. Bayclone: Bayesian nonparametric inference of tumor subclones using NGS data. In *Pacific Symposium on Biocomputing Co-Chairs*, pages 467–478. World Scientific, 2014. doi: 10.1142/9789814644730_0044. [p2]

E. Sollier, J. Kuipers, K. Takahashi, N. Beerenwinkel, and K. Jahn. COMPASS: joint copy number and mutation phylogeny reconstruction from amplicon single-cell sequencing data. *Nature communications*, 14(1):4921, 2023. doi: 10.1038/s41467-023-40378-8. [p2]

F. Strino, F. Parisi, M. Micsinai, and Y. Kluger. TrAp: a tree approach for fingerprinting subclonal tumor composition. *Nucleic Acids Research*, 41:e165 – e165, 2013. doi: 10.1093/nar/gkt641. [p1]

G. Tanner, D. R. Westhead, A. Droop, and L. F. Stead. Simulation of heterogeneous tumour genomes with heterogenesis and in silico whole exome sequencing. *Bioinformatics*, 35(16): 2850–2852, 2019. doi: 10.1093/bioinformatics/bty1063. [p2]

J. Wu and M. El-Kebir. ClonArch: visualizing the spatial clonal architecture of tumors. *Bioinformatics*, 36(Supplement_1):i161–i168, 2020. doi: 10.1093/bioinformatics/btaa471. [p2]

K. Yuan, T. Sakoparnig, F. Markowetz, and N. Beerenwinkel. BitPhylogeny: a probabilistic framework for reconstructing intra-tumor phylogenies. *Genome Biology*, 16(1):1–16, 2015. doi: 10.1186/s13059-015-0592-6. [p2]

Aitor Sánchez-Ferrera
Intelligent Systems Group, Computer Science Faculty, University of the Basque Country
Paseo Manuel Lardizabal, Donostia/San Sebastian, 20018
Spain
ORCiD: 0000-0001-6127-0686
aitor.sanchezf@ehu.eus

Maitena Tellaetxe-Abete
Intelligent Systems Group, Computer Science Faculty, University of the Basque Country
Paseo Manuel Lardizabal, Donostia/San Sebastian, 20018
Spain
ORCiD: 0000-0003-1894-4547
maitena.tellaetxe@ehu.eus

Borja Calvo-Molinos
Intelligent Systems Group, Computer Science Faculty, University of the Basque Country
Paseo Manuel Lardizabal, Donostia/San Sebastian, 20018
Spain
ORCiD: 0000-0001-9969-9664
borja.calvo@ehu.eus